

Achieving the ultimate optical resolution

MARTIN PAÚR,¹ BOHUMIL STOKLASA,¹ ZDENEK HRADIL,¹ LUIS L. SÁNCHEZ-SOTO,^{2,3,*} AND JAROSLAV REHACEK¹

¹Department of Optics, Palacký University, 17. listopadu 12, 771 46 Olomouc, Czech Republic

²Departamento de Óptica, Facultad de Física, Universidad Complutense, 28040 Madrid, Spain

³Max-Planck-Institut für die Physik des Lichts, Günther-Scharowsky-Straße 1, Bau 24, 91058 Erlangen, Germany

*Corresponding author: lsanchez@fis.ucm.es

Received 6 July 2016; revised 31 August 2016; accepted 3 September 2016 (Doc. ID 269908); published 12 October 2016

The Rayleigh criterion specifies the minimum separation between two incoherent point sources that may be resolved into distinct objects. We revisit this problem by examining the Fisher information required for resolving the two sources. The resulting Cramér–Rao bound gives the minimum error achievable for any unbiased estimator. When only the intensity in the image plane is recorded, this bound diverges as the separation between the sources tends to zero, an effect that has been dubbed the Rayleigh curse. Nonetheless, this curse can be lifted with suitable measurements. Here, we work out optimal strategies and present a realization for Gaussian and slit apertures, which is accomplished with digital holographic techniques. Our results confirm immunity to the Rayleigh curse and an unprecedented experimental precision. © 2016 Optical Society of America

OCIS codes: (100.6640) Superresolution; (110.3055) Information theoretical analysis; (270.5585) Quantum information and processing.

<http://dx.doi.org/10.1364/OPTICA.3.001144>

Optical resolution is a measure of the ability of an imaging system to resolve spatial details in a signal. As realized long ago [1], this resolution is fundamentally determined by diffraction, which smears out the spatial distribution of light so point sources map onto finite spots at the image plane. This information is aptly encompassed by the point-spread function (PSF) [2].

The diffraction limit was deemed an unbreakable rule, nicely epitomized by the time-honored Rayleigh criterion [3]: points can be resolved only if they are separated by at least the spot size of the PSF of the imaging system.

The conventional means by which one can circumvent this obstruction are to reduce the wavelength or to build higher numerical-aperture optics, thereby making the PSF narrower. In recent years, though, several intriguing approaches have emerged that can break this rule under certain special circumstances [4–10]. Despite their success, these techniques are often involved and require careful control of the source, which is not always possible in every application.

Quite recently, a groundbreaking proposal [11–13] has re-examined this question from the alternative perspective of quantum metrology. The chief idea is to use the quantum Fisher

information to quantify how well the separation between two poorly resolved incoherent point sources can be estimated. The associated quantum Cramér–Rao lower bound (qCRLB) gives a bound on the accuracy of that estimation. Surprisingly enough, the qCRLB maintains a fairly constant value for any separation of the sources, which implies that the Rayleigh criterion is secondary to the problem at hand.

In this Letter, we elaborate on this issue, presenting quite a straightforward way of determining the ultimate resolution limit. More importantly, we find the associated optimal measurement schemes that attain the qCRLB. We study examples of Gaussian and sinc PSFs and implement our new method in a compact and reliable setup. For distances below the Rayleigh limit, the uncertainty of this measurement is much less than with direct imaging.

Let us first set the stage for our simplified model. We follow Lord Rayleigh’s lead and assume quasimonochromatic paraxial waves with one specified polarization and one spatial dimension, x denoting the image-plane coordinate. To facilitate possible generalizations, we phrase what follows in a quantum parlance. This is justified because wave optics and quantum mechanics share the same mathematical structure. With this in mind, a wave of complex amplitude $U(x)$ can be assigned to a ket $|U\rangle$, such that $U(x) = \langle x|U\rangle$, where $|x\rangle$ is a vector describing a point-like source at x .

Moreover, we consider a spatially invariant unit-magnification imaging system characterized by its PSF, which represents its normalized intensity response to a point light source. We shall denote this PSF as $I(x) = |\langle x|\psi\rangle|^2 = |\psi(x)|^2$.

Two incoherent point sources are imaged by that system. For simplicity, we consider them to have equal intensities and to be located at two unknown points $X_1 = \varepsilon/2$ and $X_2 = -\varepsilon/2$ of the object plane. The task is to give a sensible estimate of the separation $\varepsilon = X_1 - X_2$. The relevant coherence matrix, which embodies the image-plane modes, can be jotted down as

$$e_{\varepsilon} = \frac{1}{2}(|\psi_1\rangle\langle\psi_1| + |\psi_2\rangle\langle\psi_2|), \quad (1)$$

where $|\psi_1\rangle = \exp(iP\varepsilon/2)|\psi\rangle$ (and an analogous expression for $|\psi_2\rangle$), and P is the momentum operator (in units $\hbar = 1$ throughout) that generates displacements in the x variable. In the x -representation, e_{ε} appears as the normalized mean intensity profile, which is the image of spatially shifted PSFs; namely,

$q_{\mathfrak{s}}(x) = \frac{1}{2}(|\psi(x - \mathfrak{s}/2)|^2 + |\psi(x + \mathfrak{s}/2)|^2)$. This confirms that the momentum acts as a derivative $P = -i\partial_x$.

For points close enough together, ($\mathfrak{s} \ll 1$), which we shall assume henceforth, a linear expansion gives

$$|\psi_1\rangle = \mathcal{N}(1 + iP\mathfrak{s}/2)|\psi\rangle, \quad |\psi_2\rangle = \mathcal{N}(1 - iP\mathfrak{s}/2)|\psi\rangle, \quad (2)$$

where $\mathcal{N} = [1 + \langle\psi|P^2|\psi\rangle\mathfrak{s}^2/4]^{-1/2}$ is a normalization constant. The crucial point is that $\langle\psi_2|\psi_1\rangle \neq 0$, so the spatial modes excited by the two sources are not orthogonal, in general. This overlap is at the heart of all the difficulties of the problem, for it implies that the two modes cannot be separated by independent measurements.

To bypass this problem, we bring in the symmetric (+) and antisymmetric (-) states

$$\begin{aligned} |\psi_+\rangle &= C_+(|\psi_1\rangle + |\psi_2\rangle) \simeq |\psi\rangle, \\ |\psi_-\rangle &= C_-(|\psi_1\rangle - |\psi_2\rangle) \simeq \frac{P|\psi\rangle}{\sqrt{\langle\psi|P^2|\psi\rangle}}, \end{aligned} \quad (3)$$

where C_+ and C_- are normalization constants. When $\langle\psi|P|\psi\rangle = 0$, these modes are orthogonal. This happens when, e.g., the PSF is inversion symmetric, which encompasses most of the cases of interest. The modes in Eq. (3) constitute a natural set for writing the coherence matrix. Actually, in this set, $q_{\mathfrak{s}}$ is diagonal $q_{\mathfrak{s}}|\psi_j\rangle = p_j|\psi_j\rangle$, with eigenvalues $p_- = \langle\psi|P^2|\psi\rangle\mathfrak{s}^2/4$ and $p_+ = 1 - p_-$.

With our formalism, the quantum estimation theory can be directly applied to problems of classical optics. The pivotal quantity is the quantum Fisher information [14], which is a mathematical measure of the sensitivity of an observable quantity (the PSF) to changes in its underlying parameters (emitters position). It is defined as $\mathcal{F} = \text{Tr}[q_{\mathfrak{s}}L_{\mathfrak{s}}^2]$, where the symmetric logarithmic derivative $L_{\mathfrak{s}}$ is the self-adjoint operator satisfying $\frac{1}{2}(L_{\mathfrak{s}}q_{\mathfrak{s}} + q_{\mathfrak{s}}L_{\mathfrak{s}}) = \partial q_{\mathfrak{s}}/\partial\mathfrak{s}$ [15]. A direct calculation finds that

$$\mathcal{F} = 2\left[\frac{1}{p_-}\langle\psi_-|\frac{\partial q_{\mathfrak{s}}}{\partial\mathfrak{s}}|\psi_-\rangle + \frac{1}{p_+}\langle\psi_+|\frac{\partial q_{\mathfrak{s}}}{\partial\mathfrak{s}}|\psi_+\rangle\right] \simeq \langle\psi|P^2|\psi\rangle, \quad (4)$$

and \mathcal{F} turns out to be independent of \mathfrak{s} .

The associated CRLB (the qCRLB) ensures that the variance of any unbiased estimator $\hat{\mathfrak{s}}$ of the quantity \mathfrak{s} is then bounded by the reciprocal of the Fisher information; viz,

$$(\Delta\hat{\mathfrak{s}})^2 \geq \frac{1}{\mathcal{F}} = \frac{1}{\langle\psi|P^2|\psi\rangle}. \quad (5)$$

As this accuracy remains also constant, considerable improvement can be obtained if an optimal measurement, saturating Eq. (5), is implemented. We stress that although this ultimate resolution follows from the qCRLB, the quantum nature of light plays no role.

Before we proceed further, we make a pertinent remark. The Fisher information for standard image-plane intensity detection (or photon counting, in the quantum regime) reads as

$$\mathcal{F}_{\text{std}} = \int_{-\infty}^{\infty} \frac{1}{q_{\mathfrak{s}}(x)} \left[\frac{\partial q_{\mathfrak{s}}(x)}{\partial\mathfrak{s}}\right]^2 dx. \quad (6)$$

Performing again a first-order expansion in \mathfrak{s} , \mathcal{F}_{std} can be expressed in terms of the PSF $I(x)$:

$$\mathcal{F}_{\text{std}} \simeq \mathfrak{s}^2 \int_{-\infty}^{\infty} \frac{[I''(x)]^2}{I(x)} dx. \quad (7)$$

Now, \mathcal{F}_{std} goes to zero quadratically as $\mathfrak{s} \rightarrow 0$. This means that, in this standard strategy, detecting the intensity becomes progressively worse at estimating the separation for closer sources, to the point that the standard CRLB diverges at $\mathfrak{s} = 0$. This divergent behavior has been termed the *Rayleigh curse* [11]. In other words, there is much more information available about the separation of the sources in the phase of the field than in the intensity alone.

From our previous discussion, it is clear that the projectors $\Pi_j = |\psi_j\rangle\langle\psi_j|$ ($j = +, -$) comprise the optimal measurements of the parameter $\mathfrak{s} \ll 1$ [16]. Notice that in Eq. (4), the antisymmetric mode p_- gives the leading contribution, and thus, most useful information can be extracted from the Π_- channel. As a consequence, the wave function of the optimal measurement becomes

$$\psi_{\text{opt}}(x) = \langle x|\psi_-\rangle = \frac{\psi'(x)}{\sqrt{\mathcal{F}}}, \quad (8)$$

where

$$\mathcal{F} = \langle\psi|P^2|\psi\rangle = \int_{-\infty}^{\infty} [\psi'(x)]^2 dx. \quad (9)$$

Let us consider two relevant examples of PSFs, the Gaussian and the sinc,

$$\begin{aligned} \psi^G(x) &= \frac{1}{(2\pi\sigma^2)^{\frac{1}{4}}} \exp\left(-\frac{x^2}{4\sigma^2}\right), \\ \psi^S(x) &= \frac{1}{\sqrt{w}} \frac{\sin(\pi x/w)}{\pi x/w}, \end{aligned} \quad (10)$$

where σ and w are effective widths that depend on the wavelength. From Eq. (9) it is straightforward to obtain the quantum Fisher information for these two cases: $1/(4\sigma^2)$ and $\pi^2/(3w^2)$. The optimal measurements are then

$$\begin{aligned} \psi_{\text{opt}}^G(x) &= \frac{-1}{(2\pi)^{\frac{1}{4}}\sigma^{\frac{3}{2}}} x \exp\left(-\frac{x^2}{4\sigma^2}\right), \\ \psi_{\text{opt}}^S(x) &= \sqrt{3} \left[\frac{w^{\frac{1}{2}}}{\pi x} \cos\left(\frac{\pi x}{w}\right) - \frac{w^{\frac{3}{2}}}{\pi^2 x^2} \sin\left(\frac{\pi x}{w}\right) \right]. \end{aligned} \quad (11)$$

To project on these functions, one needs to separate the image-plane field in terms of the desired spatial modes. This has been implemented in our laboratory with the setup sketched in Fig. 1. Two incoherent point-like sources were generated by a digital light projector (DLP) Lightcrafter evaluation module (Texas Instruments), which uses a digital micromirror chip (DMD) with square micromirrors of 7.6 μm size each. This allows for precise control of the points separation by individually addressing two particular micromirrors. The DMD chip was illuminated by an intensity-stabilized He-Ne laser equipped with a beam expander to get a sufficiently uniform beam. The spatial incoherence is ensured by switching between the two object points so that only one was ON at a time, keeping the switching time well below the detector time resolution.

The two point sources were imaged by a low numerical-aperture lens and shaped by an aperture placed behind the lens. A circular diaphragm produced Airy rings, but these are well approximated by a Gaussian PSF. The sinc PSF was obtained by inserting a squared slit. We experimentally measured the values

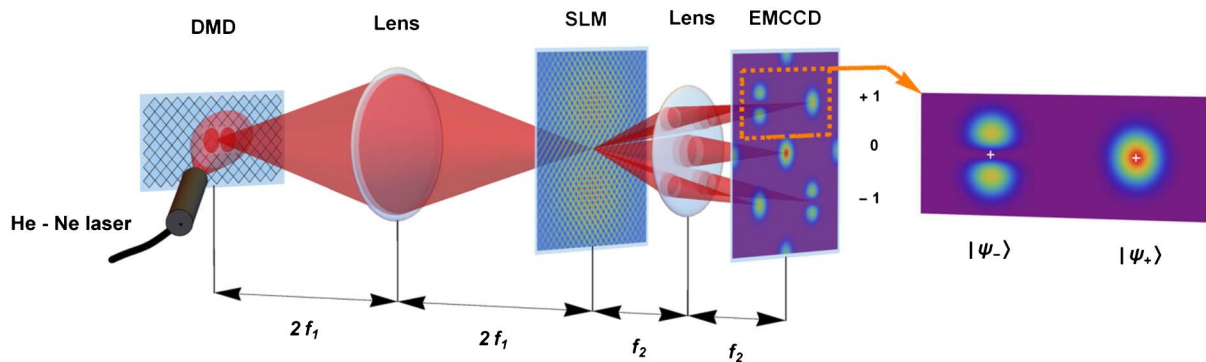


Fig. 1. Schematic diagram of the experimental setup. Two incoherent point sources are created with a high frequency switched digital micromirror chip (DMD) illuminated with an intensity-stabilized He–Ne laser. The sources are imaged by a low-aperture lens. In the image plane, projection onto different modes is performed with a digital hologram created with an amplitude spatial light modulator (SLM). Information about the desired projection is carried by the first-order diffraction spectrum, which is mapped by a lens onto an EMCCD camera.

$\sigma = 0.05$ mm and $w = 0.15$ mm. The Rayleigh criteria for these values are 2.635σ and w , respectively. For Gaussian PSFs, we somewhat arbitrarily define the Rayleigh criterion to be the separation for which the maximum drop of intensity between the two images quantified by $I(0)/[\max I(x)]$ equals that of two Rayleigh-distance separated sinc PSFs ($\approx 81\%$). The two-point separations ε were varied in steps of 0.01 mm, which corresponds to steps 0.2σ for the Gaussian and $0.067w$ for the sinc. The smallest separations attained are 13 times smaller than the Rayleigh limit for the Gaussian and 10 times for the sinc.

The projection onto any basis is performed with a spatial light modulator (CRL OPTO) in the amplitude mode. We prepare a hologram at the image plane produced as an interference between a tilted reference plane wave and the desired projection function ψ_{opt} . When this is illuminated by the two-point source, the intensity in the propagation direction of the reference wave is

$$\left| \int_{-\infty}^{\infty} \psi_{\text{opt}}^*(x) \psi(x + \varepsilon/2) dx \right|^2 + \left| \int_{-\infty}^{\infty} \psi_{\text{opt}}^*(x) \psi(x - \varepsilon/2) dx \right|^2. \quad (12)$$

Different projections can be obtained with different reference waves.

To prepare the hologram, the nominal PSF parameters (σ and w) were measured in advance. For the Gaussian PSF, we prepared projection on both the zeroth- and first-order Hermite–Gaussian modes. The measurement of the zeroth-order mode is used to assess the total number of photons in each measurement run. For the sinc, the image was also projected on the PSF itself and its first spatial derivative.

The desired projection is carried by the first diffraction order. To get the information, the signal is Fourier transformed by a short focal lens and detected by a cooled electron-multiplying CCD (EMCCD) camera (Raptor Photonics) working in the linear mode with on-chip gain g to suppress the effects of read-out noise and dark noise. As sketched in Fig. 1, the outcome of a measurement consists of two photon counts detected from the Fourier spectrum points representing spatial frequencies connected with the reference waves. These data carry information about the separation of the two incoherent point sources.

The noise from a final number of detection events is further increased by the excess noise due to the random nature of the EMCCD gain, the background noise caused by the scattered

photons reaching the detector, and by slight misalignments of the SLM hologram with respect to the two-point image. While the excess camera noise tends to increase the measurement errors uniformly across the measured range of separations, the constant background noise affects mostly the smallest separations. For those, the signal—the intensity of the antisymmetric projection—is weak, and the background photons make considerable contributions.

The numbers of photons n_0 and n_- detected in the PSF $|\psi\rangle$ and antisymmetric (optimal) modes $|\psi_-\rangle$, respectively, was determined by using the EMCCD pixel capacity and g . The relative frequency of measuring the antisymmetric projection was calculated as $f_- = n_- / (n_0 + n_-)$, the denominator $n_0 + n_-$ being roughly the total number of detected photons. The estimator of the separation is then obtained by solving the relation $f_- = \langle \psi_- | \rho_\varepsilon | \psi_- \rangle$ for ε . We make no assumption about the smallness of ε , which helps to produce unbiased estimates of larger separations.

To determine estimator characteristics, 500 measurements for each separation were carried out. The results are summarized in Fig. 2. The optimal method overcomes the direct position measurement for small and moderate separations. For the Gaussian PSF (left panel) and the smallest separation 0.2σ , the experimental mean squared estimator (MSE) is $2.35 \times \text{qCRLB}$; i.e., more than 20 times smaller than the error of the position measurement ($51.2 \times \text{qCRLB}$). For the sinc, the experimental MSE is $2.23 \times \text{qCRLB}$ for the smallest separation, which is 4.5 times lower than the error of the position measurement ($10.1 \times \text{qCRLB}$).

Two different effects increase the error slightly above the theoretical limit. For small and moderate separations, the background and excess noise discussed above become important. For large separations, the two-mode measurement derived in this paper is no longer optimal. However, in this regime, the direct CCD imaging becomes nearly optimal, so any measurement setup attaining the theoretical limit would bring about only marginal improvement with respect to the simple CCD detection. We mention in passing that the optimal measurement of the sinc PSF is more challenging due to very fast oscillations of the PSF derivative. Nevertheless, the results are quite satisfactory.

In summary, we have developed and demonstrated a simple technique that surpasses traditional imaging in its ability to

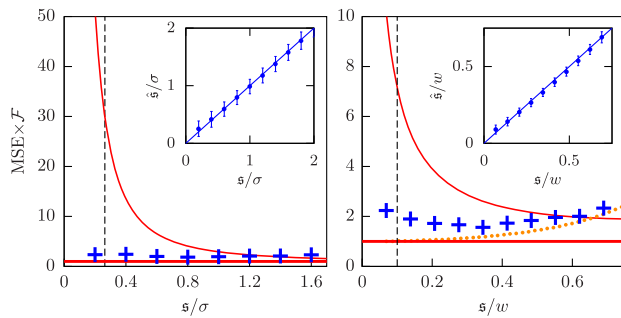


Fig. 2. Mean-square error of the estimated separation for Gaussian (left panel) and sinc (right panel) PSFs. Separations are expressed in units of PSF widths σ and w and the MSE in units of the qCRLB. The main graph compares the performance of our experimental method (blue symbols) with the theoretical lower bound for the CCD measurement (thin red curve) and the ultimate limit (thick red line). The vertical dotted lines delimit the 10% of the Rayleigh limit for each PSF. The insets show the statistics of the experimental estimates. Mean values are plotted in blue dots with standard deviation bars around. The true values are inside the standard deviation intervals for all separations and the estimator bias is negligible. For the two largest measured separations, the experimental MSE nicely follows the CRLB calculated for the experimentally realized antisymmetric projection (orange dots).

resolve two closely spaced point sources. The method does not require any exotic illumination and is applicable to classical incoherent sources. Much in the spirit of the original proposal [11–13], our results stress that diffraction resolution limits are not a fundamental constraint but, instead, the consequence of traditional imaging techniques discarding the phase information.

Moreover, our treatment also suggests other directions of research. Whereas the point source represents a natural unit for image processing (upon which hinges the very definition of PSF), other “signal units” can be further expanded and processed in a similar way. Optimal detection can then be tailored to suit the desired target. This clearly provides a novel and not yet explored avenue for image-processing protocols. We firmly believe that this approach will have a broad range of applications in the near future.

Note: While preparing this manuscript, we came to realize that similar conclusions, although with different techniques, were

being reached by Sheng *et al.* [17], Yang *et al.* [18], and Tham *et al.* [19].

Funding. Grantová Agentura České Republiky (GACR) (TE01020229); Technologická Agentura České Republiky (TA CR) (15-03194S); Univerzita Palackého v Olomouci (UP) (IGA PrF 2016-005); Ministerio de Economía y Competitividad (MINECO) (FIS2015-67963-P).

Acknowledgment. We thank Gerd Leuchs, Robert Boyd, Olivia Di Matteo, and Matthew Foreman for the valuable discussions and comments. The encouraging exchanges with Mankei Tsang are also appreciated.

REFERENCES

1. E. Abbe, *Arch. Mikrosk. Anat.* **9**, 469 (1873).
2. J. W. Goodman, *Introduction to Fourier Optics* (Roberts & Company, 2004).
3. L. Rayleigh, *Philos. Mag.* **8**, 261 (1879).
4. *Nat. Photonics* **3**, 361 (2009).
5. S. W. Hell, *Science* **316**, 1153 (2007).
6. M. I. Kolobov, “Quantum limits of optical super-resolution,” in *Quantum Imaging* (Springer, 2007), pp. 113–138.
7. S. W. Hell, *Nat. Methods* **6**, 24 (2009).
8. G. Patterson, M. Davidson, S. Manley, and J. Lippincott-Schwartz, *Annu. Rev. Phys. Chem.* **61**, 345 (2010).
9. A. J. den Dekker and A. van den Bos, *J. Opt. Soc. Am. A* **14**, 547 (1997).
10. C. Cremer and B. R. Masters, *Eur. Phys. J. H* **38**, 281 (2013).
11. M. Tsang, R. Nair, and X.-M. Lu, *Phys. Rev. X* **6**, 031033 (2016).
12. R. Nair and M. Tsang, “Ultimate quantum limit on resolution of two thermal point sources,” arXiv:16004.00937.
13. S. Z. Ang, R. Nair, and M. Tsang, “Quantum limit for two-dimensional resolution of two incoherent optical point sources,” arXiv:1606.00603.
14. L. Motka, B. Stoklasa, M. D’Angelo, P. Facchi, A. Garuccio, Z. Hradil, S. Pascazio, F. V. Pepe, Y. S. Teo, J. Rehacek, and L. L. Sanchez-Soto, *Eur. Phys. J. Plus* **131**, 130 (2016).
15. D. Petz and C. Ghinea, *Introduction to Quantum Fisher Information* (World Scientific, 2011), Vol. **27**, pp. 261–281.
16. C. Lupo and S. Pirandola, “Ultimate precision limits for quantum sub-Rayleigh imaging,” arXiv:1604.07367.
17. T. Z. Sheng, K. Durak, and A. Ling, “Fault-tolerant and finite-error localization for point emitters within the diffraction limit,” arXiv:1605.07297.
18. F. Yang, A. Tashilina, E. S. Moiseev, C. Simon, and A. I. Lvovsky, “Far-field linear optical superresolution via heterodyne detection in a higher-order local oscillator mode,” arXiv:1606.02662.
19. W. K. Tham, H. Ferretti, and A. M. Steinberg, “Beating Rayleigh’s curse by imaging using phase information,” arXiv:1606.02666.